Accepted Manuscript.
Article accepted for publication in Ocean Engineering, 22/11/2019.

The effect of rope termination on the performance of polyester mooring ropes for marine applications

Hossein Saidpour[a], Liang Li[a*], Rahim Vaseghi[b]

[a]School of Engineering and Computer Science, University of Hertfordshire, Herts, AL10 9AB, UK

[b]Islamic Azad University, Knowledge Village Dubai, Dubai, United Arab Emirates

Abstract

Termination of heavy-duty polyester mooring ropes has long been an issue of concern in the marine renewable energy applications. In this study, experimental investigations were conducted on two different rope materials to investigate and compare the performance of filament, yarn, strand, sub-rope, 44mm rope and 120mm rope. The experiment setup consisted of 5kN Lloyds Machine for testing filament, yarn and strand, 500kN Denison Machine for sub-rope, 1500kN and 30MN tensile equipment for testing 44mm and 120mm ropes respectively. At constant test conditions, extensive experiments were carried out to examine the effects of various termination configuration on rope performance. The terminations used included Parafil socket (Viking 7 socket), splice and another novel termination called Stress Relief Socket. The results show that the use of stress relief socket has led to increased tensile performance of existing ropes by up to 13% for Akzo ropes. Considering the results of the tensile tests, the Stress Relief Socket has proved to have a significant advantage for replacement of existing methods of termination e.g. the splice. It should also be noted that the reproduction of the socket termination is more consistent than that of other methods of termination. The experimental outcomes can instruct future optimal mooring system design and marine renewable energy performances.

Keywords: polyester mooring rope; rope termination; tensile testing; marine renewable energy.

*Corresponding author. Tel.: +44(0) 1707284151.

E-mail address: l.li30@herts.ac.uk (L.Li).

Nomenclature

BL	Breaking Load	OSD	Off Side Displacement transducers
D	Diameter	R	Resin
E	Extension to break	T	Tenacity
FS	Full Spike	T_i	Filament Tenacity
H	Heatshrink	T_R	Sample Tenacity
HS	Half Spike	ΔL_{rope}	Total extension in the rope
L_t	Transducer distance	ΔL_{SD}	Socket draw
L_{total}	Sample length (socket face to socket face)	ΔL_{MD}	Machine displacement
MD	Machine Displacement	η	The Construction Efficiency
NSD	Near Side Displacement transducers	ε_{total}	Total strain in the rope

1. Introduction

Most floating marine renewable energy (MRE) components need mooring systems, in order to maintain the components on station and provide resilience to offset the combined effects of current loads, waves and wind. Wire rope and steel chain have traditionally been used in MRE mooring systems over the past two decades (Lian et al., 2018), but contemporary designs often feature polyester rope which typically have a lower cost, lightweight, the ability to reduce peak loadings and ease of handling (Bashir et al., 2017). However, periodic inspections are necessary to observe the health of these ropes in MRE mooring systems. A survey of mooring system failures has been shown by the Health and Safety Executive (HSE) report (2006). According to the data during 1980 and 2018, a floating production unit will experience a mooring system failure every 9 years on average (Rivera et al., 2018). Furthermore, the one of the most common failure probability seen in the mooring systems of floating MRE units is the failure of individual polyester rope with termination (Zhang et al., 2016). The factors, which adversely affect the life of polyester rope in marine services, include environmental factors (moisture, oxygen, heat etc.), physical factors (molecular structure, specific gravity and physical structure etc.), mechanical factors (overload, creep, stress rupture etc.) and termination (Lian et al., 2017). Investigations are being carried out to assess the causes of failure in rope and the more sensitive elements in a mooring line (Singh et al., 2016). Tension Technology International (TTI) has participated in almost a thousand break tests of fibre ropes and have analysed many rope failures. TTI has investigated three major towing accidents. One involved the use of two tugs towing a platform. Computer analyses examined on the failed mooring lines. In most cases it has been proved that mooring loads exceeded the strength of the failed component (Mousavi et al., 2013). In addition, an extensive work to investigate the performance of nylon 6 fibre mooring ropes for marine renewable energy have been reviewed by Weller (Weller et al., 2015).

Ropes and chains are bodies for mooring system, whose symmetrical, mostly circular cross sections, are small compared with their lengths. They are able to transfer loads only along their axes. They cannot transfer bending moments or transverse forces of any magnitude and are unstable under compressive loads, they will bend out (Lee et al., 2015). Over the last few decades, many successful structural models have been developed to predict the static tensile behaviour of ropes and its failure mechanism (Davies et al., 2015). These models often assume that spatial locations along individual strands can be described by a helix with a sinusoidal undulation in their radius direction. Thus the local strand strain can be calculated on the basis of the differential geometry of strand segments before and after the rope is stretched. Strand load is readily determined through the load strain relationship. By converting the individual strand load into the rope axial load and summing up the contributions from different strands, a load/ strain curve is generated (Wu et al., 1995).

Most of the existing literature on the rope fatigue includes wire ropes (Chaplin, 1999; Suh and Chang, 2000; Drummond et al., 2007; Paton et al., 2001; Peterka et al., 2014; Beltrán and De Vico, 2015). However, some work has been carried out on co-polymer, high modulus polyethylene, aramid and polyester fibre ropes in the past decades (Davies et al., 2011; Huang et al., 2013; Liu et al., 2014). Experiments have shown that the strength of polyester, aramid and HMEP ropes may degrade due to cyclic loading (Liu et al., 2014). The mechanism of fatigue is not fully investigated yet and cannot be accurately predicted. One factor, which may affect the fatigue rate at which the fibres are tensioned, is their position in the mooring line. Another factor is the load range over which the rope is cycled. The fatigue deterioration of a rope is a complex process. Often, as in the case of MRE components, a rope will be subjected to repetitive tensioning accompanied by free transverse motion. Although the average loading level may be less than 10% of the nominal breaking strength, the transverse motion may cause local bending, inter-strand movement, and high lateral pressure (Heirigs and Schwartz, 1992).

When some materials are subjected to permanently applied loads for MRE they eventually creep to failure. This phenomenon is generally referred to as creep-rupture (Lian et al., 2015). Weller et al. (2015) carried out a series of tests on different nylon, polyester vectran, aramid, HMPE and steel ropes under the constant and dynamic loads between 0.4% and 20% of the minimum break load. The creep curves of these rope samples showing extension versus log (time) seemed to be almost straight lines. It means that the creep-time behaviour followed a logarithmic law. During the past decades, many researchers have paid considerable attention to the creep-rupture behaviour of the Kevlar ropes (Chiao et al., 1977; Glaser et al., 1984 and Alwis and Burgoyne, 2008). In all cases it was found that Kevlar yarns would support a large proportion of their nominal short-term ultimate loadings, for long periods of time, but that there was considerable variability in the creep-rupture lifetimes for any given load level. The creep of Kevlar 49 and Kevlar 29 is generally considered to be a logarithmic function with time. The creep rates for Kevlar are low when compared with other nylon or polyester ropes, and it actually approaches that of steel. The creep rates for yarns of Kevlar 29 and Kevlar 49 are insensitive to the loads between 20% and 50% of the ultimate load but that they decrease at lower loads. Creep rates of 0.02% and 0.052% per decade were observed at room temperature for Kevlar 49 and Kevlar 29 respectively (Lafitte and Bunsell, 1982).

It is know that the performance of the combined polyester rope and termination is an important parameter in determining the cost effective design of MRE mooring systems (Weller et al., 2015; Xu et al., 2014; Gordelier et al., 2018). However, the detailed tensile performance of filament, yarn, strand, sub-rope, 44mm rope and 120mm rope needs to be further investigated. In addition, the tensile performance of a polyester rope with termination is more complicated than that of the rope only used in the MRE mooring systems. A termination can take an important role in the system design and operation but this also needs further investigation. Accordingly, this paper examines the load bearing capability of two different rope materials with differing construction and terminations. A novel termination namely Stress Relief Socket has been designed and tested. Therefore, the performance of the samples was examined under controlled environments, the ropes of different constructions and having different terminations were subjected to a specific loading condition using four different tensile test rigs, and the deformation was monitored until the final fracture was achieved. The research outcomes can contribute significantly to the polyester rope material and size selections, termination design and rope with termination performance control for MRE mooring systems.

2. Experimental facilities and testing

The specification of materials, construction of ropes and testing equipment are presented in this section. The aim of the experimental work in this study is to investigate the loading performance of different rope-termination systems for large diameter polyester ropes. In this study all the terminations were prepared manually and therefore the termination quality depends on the skillset of the personnel preparing the terminations. Hence care was taken to reduce any variability in the quality and make reproducible terminations, the same person prepared all the terminations after an extensive period of training.

2.1 Samples

Rope samples with different diameters, constructions, terminations, and materials were used. The filaments were provided from Akzo and Hoechst manufacturers. Akzo material was supplied by Akzo Noble Industrial Fibres and Hoechst 785 material was supplied by Hoechst Corp. US. The polyester material supplied by Hoechst contained a surface coating to improve the water resistance property. The difference between Hoechst and Akzo polyester grades was a shiny appearance of the Hoechst material. The microstructure of all the polyester grades supplied was semi-crystalline. This means that the fibres consisted of more oriented regions (crystalline regions) than less oriented regions (amorphous regions). The existence of both polymer chains orientation types of fibre and the size of the crystalline regions are important for improvements in fibre performance. The differences between the performances of different polyester grades originated from the processes involved in fibre production, including the adjustability of the properties to a specific application using heat treatment. The detailed construction of different samples is summarised in Table 1. The detailed rope construction is shown in Fig. 1. For the 44mm rope, to maintain the same weight for both Akzo and Hoechst ropes less Hoechst fibres were used to meet the same construction as Akzo since the basic Hoechst yarn material was heavier than Akzo. In addition, the basic construction of 120mm rope was the same as 44mm rope. However, the rope diameter was increased approximately by three times as compared with that of 44mm rope.

The construction of strands involves a twisting process of filaments whereas the sub-ropes used in this study are made by braiding the strands to form sub-ropes. The braiding process inherently restricts the extension under load, therefore the resulting elongation is reduced in relation to the tightness of the braiding structure.

Type	Terminology	Construction	Number of fibres (Akzo)	Number of fibres (Hoechst)
Filament	Collection of fibres of indefinite length provided by original suppliers	1880 dtex Akzo polyester fibres; 1220 dtex Hoechst polyester fibres	196	122
Yarn	Twist entity composed of filaments held together by twist	10x1880 dtex Akzo polyester fibres; 16x1220 dtex Hoechst polyester fibres	3,134	2,002
Strand	A twisted collection of yarns	10x8x1880 dtex + 1x4x1880 Akzo polyester fibres; 16x8x1220 dtex + 2x1x1220 Hoechst polyester fibres	16,570	15,860
18mm Sub-rope	Braided construction	12-carrier twill strands (one over 2 under 2); 18mm (diameter)	198,840	190,320
44mm Rope	Parallel collection	7 parallel sub-rope assembled together using a braided	1,391,880	1,332,240

		polyester protective jacket		
120mm Rope	Parallel collection	3×44mm rope (approx..)	4,175,640	3,996,720

Table 1. The construction of test samples.

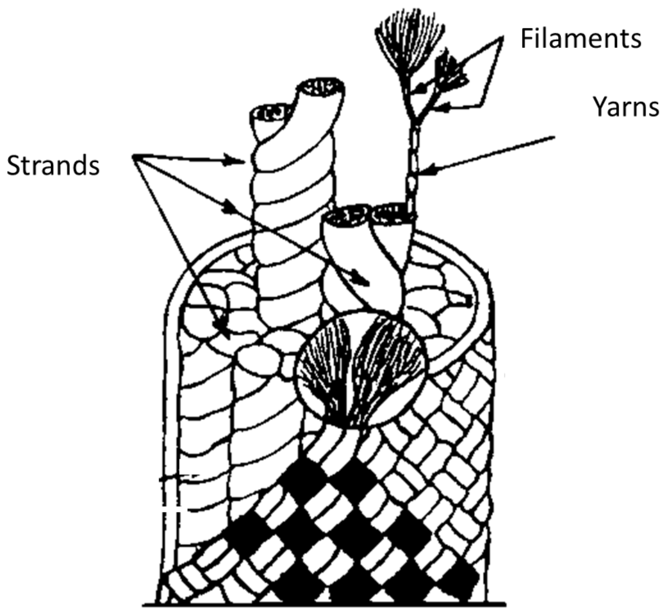

Fig.1. Schematic diagram of rope construction [Natural Disaster Organization, 1996].

2.2 Test facilities and samples preparation

Samples were taken randomly from the original spools to test filaments. Initial filament was used as the first step of the work. 1 ply filament was the original untwisted construction, which was provided by the suppliers. Different numbers of filament, up to yarn-size, were tested with 5kN Lloyds tensile machine with identical bollards, as shown in Fig. 2. The rope sample was wrapped a total of four times around the top and bottoms bollards and then clamped at each end to prevent slippage. Breaking strength, extension, tenacity and stress/strain graph were taken from the computer connected to the machine in each test. In addition, for each test, at least 12 samples of each material and construction were tested and the average value was considered to be the breaking load of the fibre. Care was taken to include only the samples which failed within the gauge length, therefore any sample with a failure in the termination vicinity were deemed to be unacceptable and therefore were excluded from the results.

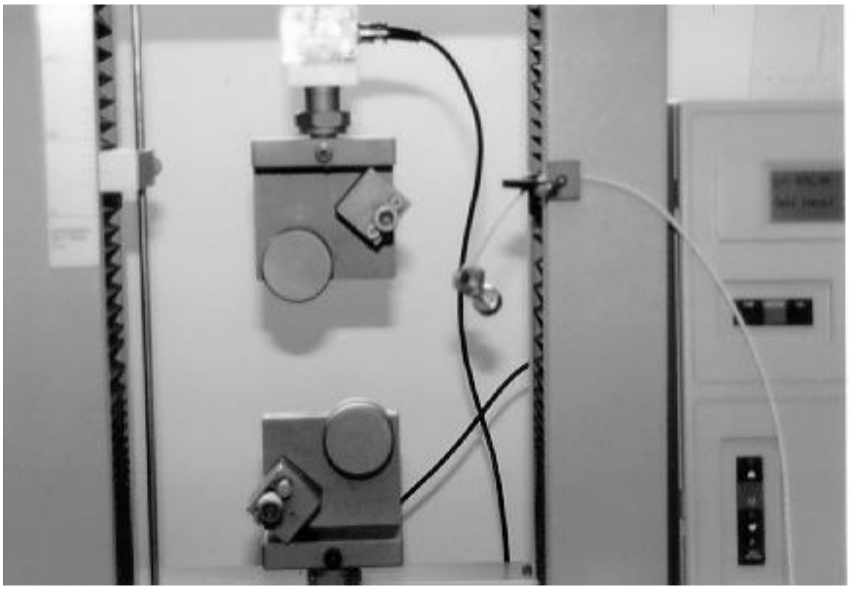

Fig. 2. 5 kN Lloyds Machine used for tensile testing of filaments, yarns and strands.

The 500kN Denison horizontal testing machine Serial No: BF1, with a load cell of 500kN was used to test the sub-ropes. Different adapters, designed to fit any termination, were used. The most usual termination was the splice, which was fitted with identical pins. The 18mm sub-rope comprised of 12 braided strands and 1.5 m long. The extra material from both sides of a sample was used to make the splice eye. The tail was turned and then inserted inside the body of rope. The tail then tapered to release tension along the rope. The buried part was taped to stop the tail from moving apart. The next method of testing was the socket. For Parafil socket, shown in Fig. 4(a), about 4m of the sub-rope was cut to make a 3m sample. The sub-rope was pulled into the socket from its nose. The yarns were opened and the socket was put inside them. Depending on the termination make up, heatshrink tubing, half socket or resin were applied. It was ascertained that the rope was passed through the heatshrink tubing before the spike was placed. A heat gun was used to shrink the heatshrink tubing. The spike and rope assembly already covered with heatshrink was then pulled back inside of the socket. To add polyester resin on the top, the socket was placed vertically. The only differences between the "Stress Relief Socket" compared with the Parafil socket, are the extra reinforcing material and changes in the socket geometry. Each sample was placed in the testing machine using identical adapters. Approximately, 30% of the initial pre-load was applied to each sample to remove any inequality/ misalignment in the strands' length, which might have occurred during the termination process. The pre-load also adjusted the spike in the socket. The tensile process was stopped before the rope broke and elongation was measured in different stages. The rope was pulled until it broke and the breaking load was considered as the ultimate strength of the rope. In every case, 12 rope samples were used.

The Digital Monitor 1500kN tensile machine was used to test the 44mm diameter ropes, as shown in Fig.3. In each case, 12 samples were tested. The testing machine was assembled in Bridon Marine, with a load cell of 1500 kN. The digital monitor locks on the highest value at failure load. Three methods of termination were used for 44mm rope, namely splice, Parafil socket and stress relief socket. To hold the assembly sockets, especial adapters were made, as the original setting could not accommodate the assembly socket. For splice, the rope comprised of 7 individual sub-ropes. Each sub-rope was spliced as an individual rope. The only precaution to follow was that each sub-rope should not be inserted into its own body because if it happens, the splice eye would bulge. Thus, when each sub-rope was spliced, pieces of rope were tied around the complete rope to keep the splice together. Viking7 socket, as shown in Fig. 4(b), is an enlargement of Parafil socket for 44mm rope because there is no socket for that size of the rope. For stress relief socket, shown in Fig. 4(c), is a new design, which incorporates reinforcement of material inside the socket. In this process, the design of Viking7 socket was changed to include extra reinforcing material. Fig. 5 shows a cross-sectional side view of stress relief socket, which includes bore, housing member, frusto-conical outer surface, frusto-conical outer surface, frusto-conical chamber, wedge member and hollow members. The internal volume of the socket was increased although the same spikes were used. Both socket assemblies were covered with a large heatshrink. Resin was added on top of both sockets to lock tight the fibres from any movement. The initial length of the sample was measured, before the final load application, a pre-load of 100kN was applied to remove any inhomogeneity in the individual ropes. Then, the sample was loaded to break and the final breaking load was recorded from the digital monitor. A total of 12 samples were used to test each termination type.

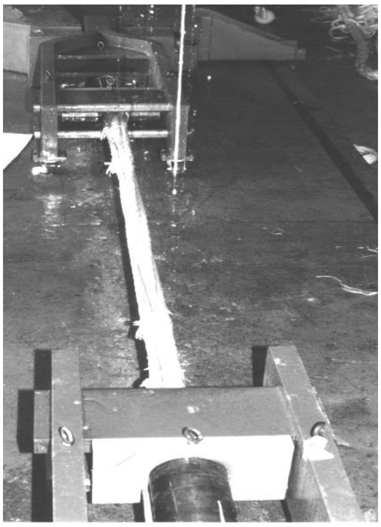

Fig.3. 44mm rope mounted in the 1500kN tensile machine used for rope testing.

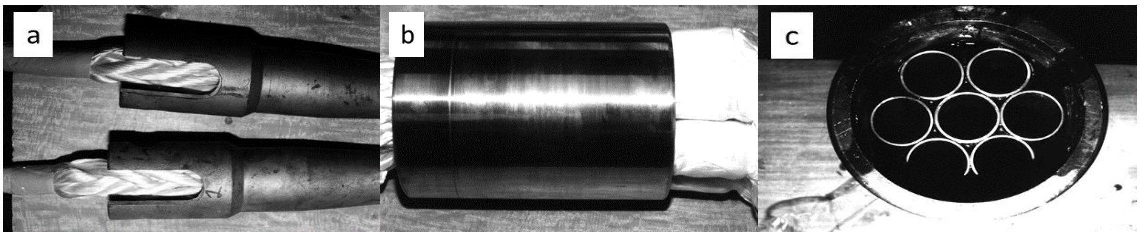

Fig. 4. Photographs of different termination with rope (a. Parafil socket, b. Viking 7 socket, c. stress relief socket)

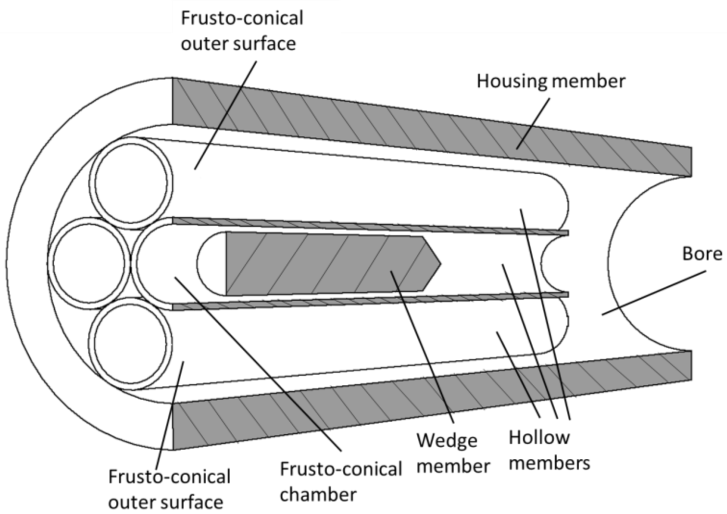

Fig. 5. A cross-sectional side view of stress relief socket.

In order to test the 120mm rope, the 30MN machine from NEL (National Engineering Laboratory in Scotland) was used, as shown in Fig. 6. This was a 30MN horizontal two-space servo hydraulic-testing machine. Eight hydraulic actuators applied a uniform force to a common moving crosshead. The applied force was derived from the summation of the transducer output and display on a digital voltmeter scaled in increments of 1 mV equivalent to 10kN. A full-scale reading of 3 volts corresponded to an applied machine force of 30MN. The procedure was the same as that for 44mm rope. However, because of the increased rope diameter, everything has been scaled up to 120mm. The initial length of each sample, stress drop during 30min holding time, extension under different loads, and breaking load were monitored by a computer.

The testing process of filaments, strands and sub ropes involved no pre-load. The elongation up to peak load and total elongation were measured using the machine LVDT sensors. However the testing of 120mm ropes involved bedding-in preload of 100 kN and the elongation was measured through machine displacement as well as two separate displacement sensors. Sample extension was measured directly using two linear transducers which were clamped to the gauge length of the rope in-between the terminations.

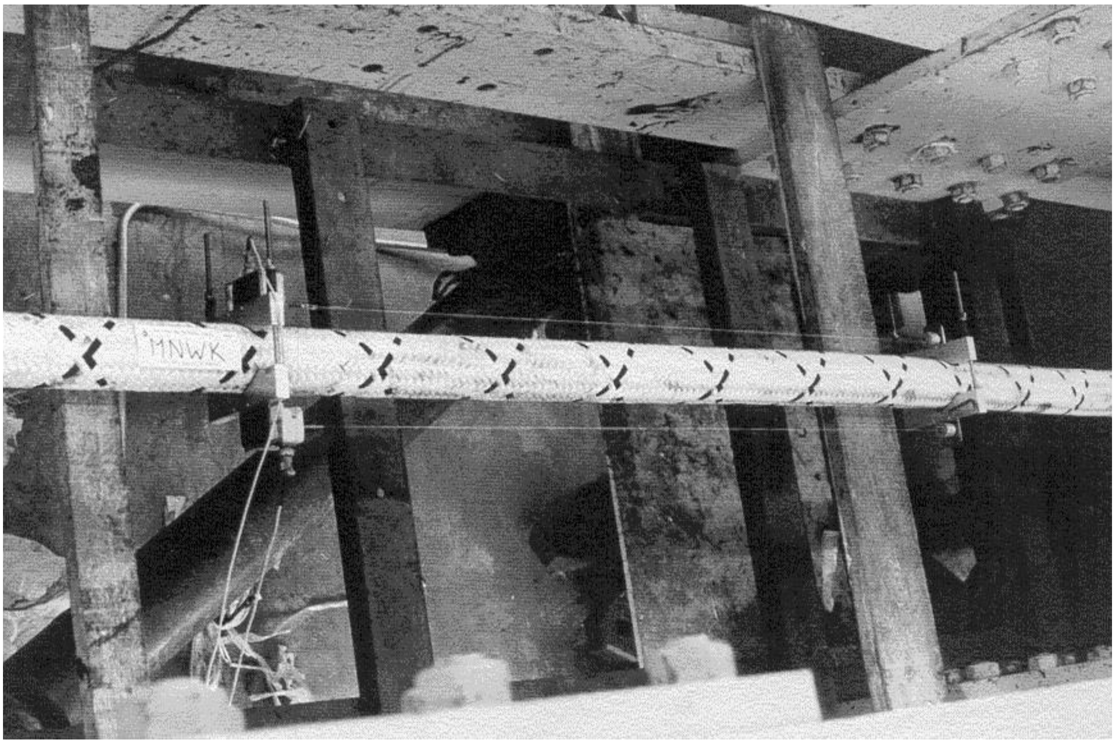

Fig. 6. The 120mm rope mounted in NEL 30MN tensile machine.

2.3 Data analysis methods

Strength or tenacity gives a measure of resistance to steady forces. It will thus be the correct quantity to consider when a specimen is subject to a steady pull, as for example, in a rope used for hosting heavy weights. The breaking elongation gives a measure of the resistance of the material to elongation. It is thus important when a specimen is subjected to stretching. All samples were tensile tested immediately after the environmental conditioning. Extension was measured from the machine cross head movement. The rope sample was wrapped a total of four times around the top and bottoms bollards and then clamped at each end to prevent slippage. The cross head speed was kept constant at 100 mm/min throughout the test. In most physical and engineering applications, load is replaced by stress. The SI unit of stress is Newton per square meter (N/m^2), which is also called a Pascal (Pa). Since the area of the cross-section is not well defined, a relationship between the mass and the load is used in the textile technology and it is called the specific stress. It is defined as following equation 1. The consistent unit for specific stress is N m/kg (or Pa m^3/kg). However, in order to fit in with Tex system for linear density, it is better to use Newton per tex (N/tex), which is 10^6 times larger than Nm/kg. For comparing different materials, the value of the specific stress at break is used and is called tenacity of specific strength.

$$Specific\ Stress = BL/Mass\ Per\ Unit\ Length \qquad (1)$$

Efficiency is simply defined as the proportion of differences between the tenacity of each sample comparted with the tenacity of initial filament divided by the tenacity of initial filament. It is calculated by following equation 2.

$$Efficiency\ \%(\sigma) = (T_R - T_i)/T_i \times 100 \qquad (2)$$

Initially load was applied for each test. It was expected to have some socket draw at this stage although pretension had been applied before. This was investigated by comparison of machine displacement with transducers. Thus, following equation 3 was used to calculate the extension of the sample:

$$E\ (\%) = 100 \times L_t/L_{total} \qquad (3)$$

After the initially load for each example, it was expected to have a long socket draw at this stage. This was investigated by comparing the machine displacement with the two transducers. It is also considered that most of the socket draw will be removed after this stage and there should be no more socket draw for the rest of the test. Thus, the socket draw can be calculated using the equation 4.

$$\Delta L_{SD} = \Delta L_{MD} - \Delta L_{total} \quad (4)$$

The total extension in the rope is calculated as following equation 5.

$$\Delta L_{rope} = \Delta L_{total} - \Delta L_{SD} \quad (5)$$

Thus, total strain in the rope can be calculated using the equation 6.

$$\varepsilon_{total} = \Delta L / L \quad (6)$$

3. Results and discussions

This section presents the main results obtained from the experiment setup in last section. Then tensile strength of different rope components was measured to investigate how it relates to different failure mechanisms. The different components tested included filament, yarn. Sub-rope and rope.

3.1 Tensile strength of filament, yarn and strand

The behaviour of filament and yarn of Akzo and Hoechst under tensile loading is shown in this part. Table 2 summarises the number of filaments, Diameter, Breaking Load, Elongation, Tenacity, and Efficiency percentage of Akzo and Hoechst filament and yarn. The results show that the most efficient filament collection consisted of 4 plies for Akzo and 8 plies for Hoechst samples with the assumption that 1 ply filament is 100% efficient. In addition, consistency in the efficiency results for Hoechst was more than that in Akzo.

<table>
<tr><th>Construction</th><th>Material</th><th></th><th>Size (Tex)</th><th>D (mm)</th><th>BL (N)</th><th>E (%)</th><th>T (mN/Tex)</th><th>η (%)</th></tr>
<tr><td rowspan="4">Untwisted 1 Ply</td><td rowspan="2">Akzo</td><td>mean</td><td>196</td><td>0.5</td><td>133</td><td>2.83</td><td>678.07</td><td>100.00</td></tr>
<tr><td>std. dev.</td><td>12</td><td>0.01</td><td>14</td><td>0.05</td><td>11</td><td>-</td></tr>
<tr><td rowspan="2">Hoechst</td><td>mean</td><td>122</td><td>-</td><td>84</td><td>1.82</td><td>692.81</td><td>100.00</td></tr>
<tr><td>std. dev.</td><td>10</td><td>-</td><td>8</td><td>0.03</td><td>11</td><td>-</td></tr>
<tr><td rowspan="4">Twisted (S) 4 Ply</td><td rowspan="2">Akzo</td><td>mean</td><td>782</td><td>0.9</td><td>520</td><td>2.69</td><td>665.53</td><td>100.77</td></tr>
<tr><td>std. dev.</td><td>70</td><td>0.01</td><td>47</td><td>0.04</td><td>12</td><td>10</td></tr>
<tr><td rowspan="2">Hoechst</td><td>mean</td><td>500</td><td>0.7</td><td>485</td><td>1.99</td><td>716.12</td><td>103.36</td></tr>
<tr><td>std. dev.</td><td>45</td><td>0.01</td><td>44</td><td>0.02</td><td>12</td><td>10</td></tr>
<tr><td rowspan="3">Twisted (S) 8 Ply</td><td rowspan="2">Akzo</td><td>mean</td><td>1554</td><td>1.25</td><td>1042</td><td>2.94</td><td>671.30</td><td>100.74</td></tr>
<tr><td>std. dev.</td><td>140</td><td>0.01</td><td>83</td><td>0.04</td><td>11</td><td>9</td></tr>
<tr><td>Hoechst</td><td>mean</td><td>1000</td><td>1.0</td><td>718</td><td>2.15</td><td>718.99</td><td>103.78</td></tr>
</table>

		std. dev.	90	0.01	57	0.02	12	9
Twisted (Z) 8 Ply	Akzo	mean	1548	1.25	1074	2.92	694.69	99.01
		std. dev.	1393	0.01	86	0.04	12	9
	Hoechst	mean	1000	1.0	731	1.96	731.99	105.66
		std. dev.	90	0.01	58	0.02	12	9
Untwisted 2x8 Ply	Akzo	mean	3120	1.90	2076	2.83	670.05	98.83
		std. dev.	250	0.01	166	0.03	10	9
	Hoechst	mean	2004	1.5	1437	2.35	717.80	103.61
		std. dev.	160	0.01	115	0.02	12	9

Table 2. Number of filaments, Diameter, Breaking Load, Elongation, Tenacity, and Efficiency percentage of Akzo and Hoechst filament and yarn.

The effects of varying extension for Akzo and Hoechst filament with different load were measured and plotted, as illustrated in Fig. 7. There is no knee region shown in both curves. Therefore, they were divided into two main parts, an initial non-linear stage, and a linear behaviour up to the break. A non-linear region for both materials started from the initial stage of load application up to 20 N and 5% extension. This non-linearity in the initial region is due to both a molecular chains reorientation within the fibres, and a reorientation of the fibres in the filaments (Davies et al., 2011) and (Bunsell, 2018). Beyond this region the curve becomes linear. The oscillations on the lateral part of loading curve in Fig 7 for Akzo filaments indicate the progression of damage resulting from fibre abrasion. The damage is caused by abrasion of filaments as a result of fibres rubbing against each other. However, the special, low friction coating on the Hoechst fibres mitigates abrasion, the curve does not show oscilations and hence prove to be more superior in achieving higher breaking load.

As shown in Table 2, Hoechst had less extension compared with Akzo at different construction. During the linear region of both filaments, Hoechst has less extension than Akzo when same load applied to both filaments.

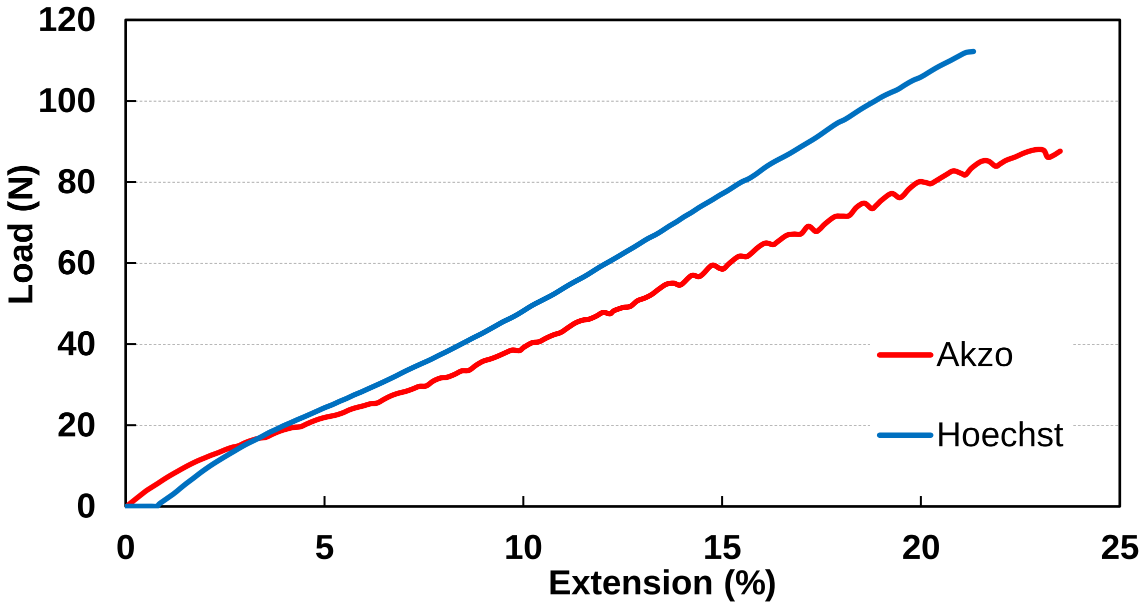

Fig. 7. Typical Load-Extension curve for Akzo and Hoechst filaments.

In addition, the effects of extension percentage of Akzo and Hoechst strands at the different applied load have all been measured and presented in Fig. 8. The dominating effect in tensile properties of strands, compared to single filament, is filament twisting, as strands are made of twisted yarns. As the load increased, the friction between the fibres leads to an increase in the heat generated. The heat will cause the fibres either to fuse together or become very compacted (Leal et al., 2017). There is a relative decrease in the rate of tenacity in both materials at similar extensions before they break which happened around 32% to 36% extension. There is a decrease in the loading properties when filaments melt. When melting, filaments tend to fuse together and behave like a uniform bar that result in increase in the final breaking tenacity. The slight irregular behaviour of the curves up to 15% extension relates to the filaments' alignment during loading and the seeming oscillation pattern towards the end of the curves indicate the extent of premature damage and failure in the individual filaments or a group of fused filaments. During the test some cracking sound was noticed before the final break. This would substantiate the oscillation or deviation of both curves from linearity towards the end during the tests. It can be seen that Hoechst strands undergo more realignment earlier in the deformation, less filament failure towards the end and superior breaking load. This is contributed to the special coating on the Hoechst filaments.

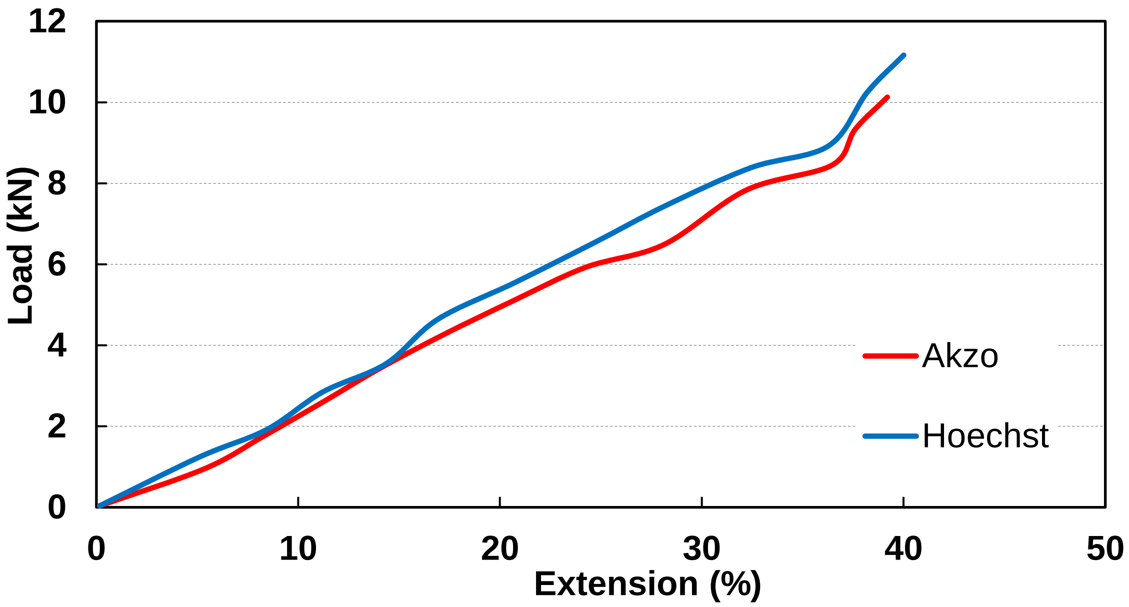

Fig. 8. Typical Load-extension curve for Akzo and Hoechst strands.

Comparison of Fig. 7 and 8 indicates some important differences in the performance of the two materials. Akzo filaments contain about 60% more fibres than Hoechst but the breaking load for Hoechst filaments is 34% higher than that of Akzo filaments. This is due to the superior abrasive resistance coating of Hoechst fibres. However, when the strands are considered the loading performance of Hoechst strands (BL=11kN) is only about 10% higher than that of Akzo strands (BL=10 kN). This is because Akzo strands contain 16570 fibres whereas Hoechst strands contain 15860 fibres, ie Akzo strands contain only 4.5% more fibres than Hoechst strands. Therefore the effect of surface coating is much less pronounced in strands.

3.2 Tensile strength of sub-rope

The reaction of fibre ropes to applied forces, energies and deformations is their most important technical property. Ropes as textile structures, react to applied stresses showing a combination of constructional and material deformation. Their reactions thus depend on the structure of the fibre material deformation used in them. Therefore, the structure of ropes is a crucial feature affecting their behaviour under applied loads. An 18 mm sub-rope of the two polyester grades, Akzo and Hoechst, were tested using three different methods of termination including Parafil, stress relief socket, and splice. Also different arrangements of spike, inside socket, were examined. In order to find out the best method of socket termination, different spike lengths and preparation were investigated. The average results of breaking load, tenacity and efficiency from Akzo & Hoechst 18mm sub-rope with Parafil socket tests with different spike lengths and preparation were measured and are summarised in Table 3. The sample configuration with Full Spike, Headshrink and Resin shows the best performance in both materials. However, half spike arrangement donates the lowest results compare to the others. This is potentially as a result of reduced contact areas between socket and spike and therefore resulting in a smaller amount of gripping properties. For the heatshrink tubing, it plays a softening role inside the socket, which allows the fibres to realign themselves when pulling. Since FS+H+R spike configuration was proved the most consistent method of termination, therefore it was selected as the testing method to measure the tensile strength for the rest of tests.

Sample Configuration		**Breaking Load (kN)**		**Tenacity (mN/Tex)**		**Efficiency (η) (%)**	
		Akzo	**Hoechst**	**Akzo**	**Hoechst**	**Akzo**	**Hoechst**
HS+H+R	mean	100.04	106.20	529.79	529.17	77.85	76.37
	std.	5	6.4	26.5	31.75	3.9	4.6

	dev.						
FS+H+R	mean	102.06	111.39	538.55	555.03	79.43	80.11
	std. dev.	5.1	6.7	26.9	33.3	3.97	4.8
FS+R	mean	101.56	108.45	535.92	540.38	79.04	77.99
	std. dev.	5.1	6.5	26.8	32.4	4	4.7

Table 3. Average data from Akzo & Hoechst 18mm sub-rope tests using different spike arrangements. (HS+H+R= Half Spike+Heatshrink+Resin; FS+H+R= Full Spike+Heatshrink+ Resin; FS+R= Full Spike+ Resin)

As mentioned in introduction, the use of different termination methods lead to significant differences in the loading performance of the sub-ropes. The average results of breaking load, tenacity and efficiency from Akzo and Hoechst 18mm sub rope under tensile load using different termination types were tested and are shown in Table 4. The stress relief socket showed an improvement in tensile property for Akzo while Hoechst showed a sharp decrease in tenacity. This loss of performance in Hoechst material is due to the incompatibility of the resin (used in the socket) with the surface coating on Hoechst fibres, which leads to fibre locking. As the stress relief socket uses more material inside the socket, fibres must have relative movement to align during the initial load application process. It has been observed that the sticky fibres cause fibre fusion followed by premature failure inside the socket.

Sample Configuration		**Breaking Load (kN)**		**Tenacity (mN/Tex)**		**Efficiency (η) (%)**	
		Akzo	**Hoechst**	**Akzo**	**Hoechst**	**Akzo**	**Hoechst**
Parafil Socket	mean	101.31	111.39	534.61	555.03	78.85	80.11

	std. dev.	4.1	5.6	21.38	27.8	3.2	4
Splice	mean	107.39	113.43	566.70	565.16	83.58	81.57
	std. dev.	4.3	5.7	22.7	28.3	3.3	4.1
Stress Relief Socket	mean	109.69	100.15	578.83	499.01	85.37	72.03
	std. dev.	4.4	5	23.2	25	3.4	3.6

Table 4. Average data from Akzo & Hoechst 18mm sub-rope tests using different termination types.

The tenacity-strain figures of the Akzo and Hoechst sub-ropes with different termination methods are graphically shown in Fig. 9. Comparison between both materials, suggests that the rope tenacity for the splice termination is less than those of Parafil and the Stress Relief sockets. The results indicate that Stress Relief Socket performs less favourably when Hoechst ropes are used; the load-extension profile of the Hoechst material in relation to splice termination is lower than that of Akzo. This is due to the application of a special coating which has been found to be incompatible with the polyester resin used in the socket to reinforce the fibres inside the socket. Whereas Akzo materials do not use any coating and therefore leads to better bond strength to the resin.

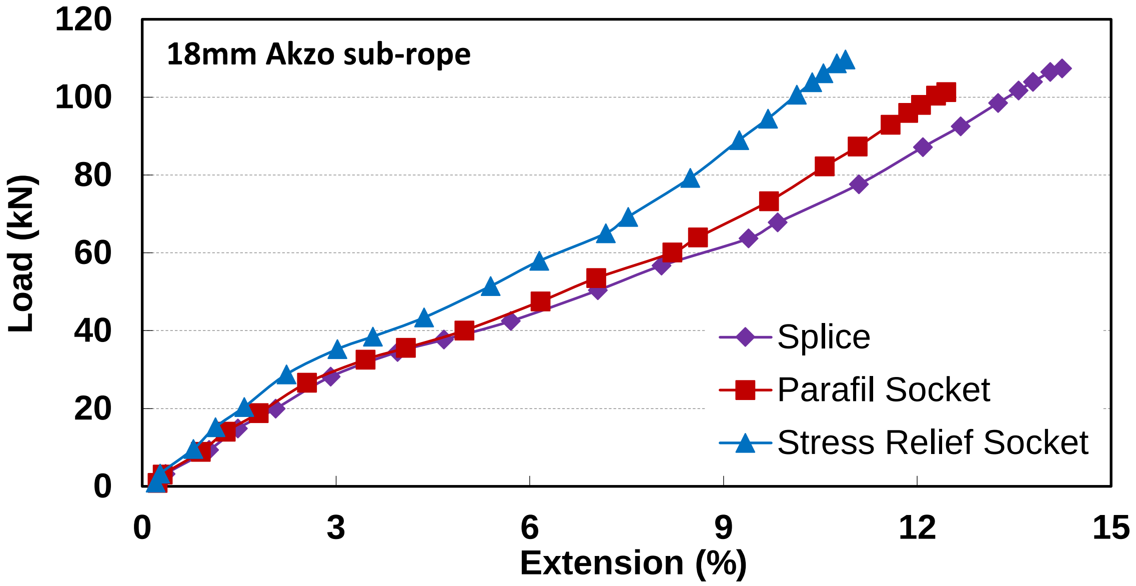

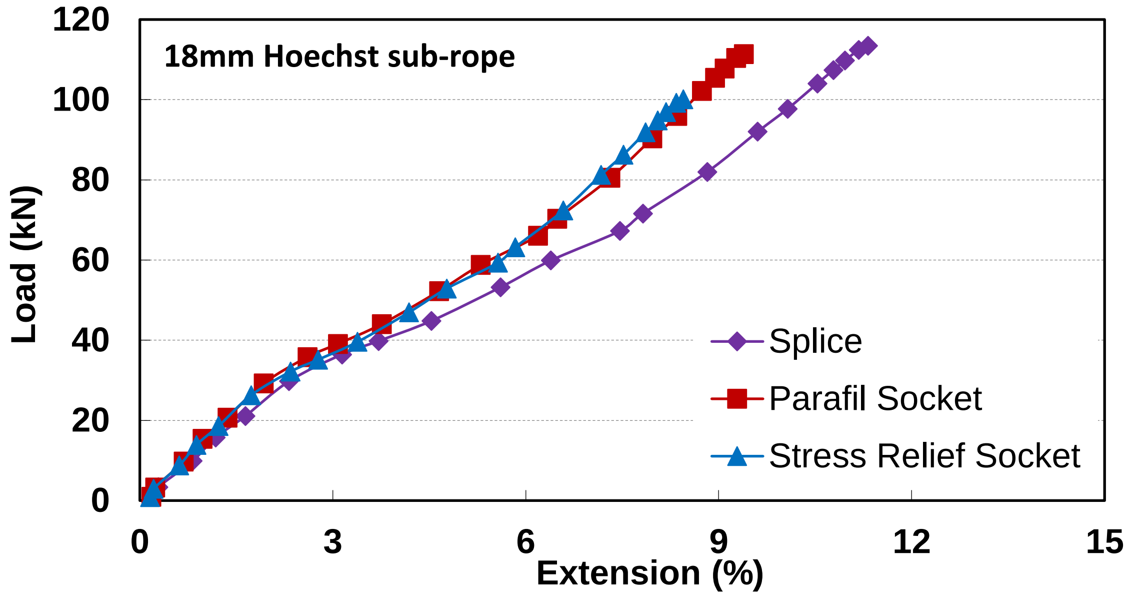

Fig. 9. Load-extension behaviour of 18mm Akzo and Hoechst sub-rope tested with different termination type.

Different termination methods have various effects on the extension to failure of sub-ropes. The extension to failure of rope using the Parafil socket was higher than that in the splice while using the Stress Relief Socket appeared to produce the lowest extension in ropes. It should be noted that extension in the Parafil and the Stress Relief socket is a combination of the socket-draw and rope extension, while in the splice slippage happens in the buried parts of the rope. It appears that the slippage in splice is smaller than the socket draw in the Parafil socket. The least rope extension occurred in the Stress Relief Socket. The main reason for this lower deformation is due to the use of extra reinforcing material within the socket, which caused fibre locking, resulting in lower extensions. In addition, the smaller socket-draw in the Stress Relief Socket is due to the stiffer and larger volume of fibre assembly inside the socket because of the extra reinforcement used. Moreover, the extension has been shown to be dependent upon the material type. The Akzo sub-rope extended 30% more than the Hoechst sub-rope under tensile loading regardless of the termination method used. The use of the Hoechst fibres in the Parafil socket led to slightly larger extensions when compared with the splice and the Stress Relief Socket.

3.3 Tensile strength of 44mm Rope

The tensile results of Akzo &Hoechst 44mm rope tested using different terminations are shown in Table 5. The normal socket was designed, to accommodate 44mm rope, based on Parafil geometry. The 44 mm rope construction also induces higher friction effects between the yarns and the terminations; this can generate premature failure at high tensile loads. Furthermore, increased diameter ropes lead to higher temperatures than within a single yarn, since the heat created by plastic deformation diffuses more slowly than in yarns. The friction phenomena can also increase the heating process. In addition, the stress concentration inside the socket is the main reason to induce failure. Failure modes of most broken samples indicated that ropes failed very close to the socket nose. This indicates that the effects of termination on failure cannot be ignored. In splice, forces are divided between the two legs that prevent failure taking place in the legs. The resulting stress concentration situated in the splice is transferred along the rope at the end of the buried part where failure usually happens. The observed mode of failure is similar in both materials, in which the failure consists of partial failure of the rope with at least one complete sub-rope failure. Complete failure of all sub-ropes is quite rare. The failure mode is highly dependent on sample preparation skills; therefore, to prepare the samples care was taken to ensure that the same method was used by the same personnel. This mode of failure has been reproducible in every sample tested, and is acceptable in the splice structures. In every case, the location for the failure is immediately after the end of the buried section of the splice where the stress concentration is high. The stress relief socket contributed the best performance for the ropes investigated. Therefore, to achieve better performance the stress concentration areas, inside the socket must be improved. This can potentially translate to better load bearing capability regardless of termination method, eg splice.

Termination Configuration		**Breaking Load (kN)**		**Tenacity (mN/Tex)**		**Efficiency (η) (%)**	
		Akzo	**Hoechst**	**Akzo**	**Hoechst**	**Akzo**	**Hoechst**
Viking 7 Socket	mean	625.24	720.45	453.07	512.77	66.82	74.01
	std. dev.	18.8	28.8	13.6	20.5	2	3
Splice	mean	669.26	779.98	484.97	555.14	71.53	80.13
	std. dev.	20.1	31.2	14.5	27.8	2.1	3.2
Stress Relief Socket	mean	753.48	819.70	546.00	583.42	80.53	84.21
	std. dev.	22.6	32.8	16.4	23.3	2.4	3.4

Table 5. Average data from Akzo & Hoechst 44mm rope tests using different termination configuration.

To compare both materials in the Stress Relief socket, a typical load-extension behaviour of the 44mm Akzo and Hoechst ropes was recorded and is shown graphically in Fig. 10. The Akzo curve showed a clear knee point before complete linear region while Hoechst tenacity pattern did not illustrate the same pattern before linear region to failure. As mentioned previously, Hoechst used a special proprietary surface coating which reduces abrasion in the fibres. This potentially reduces damage to the fibres and therefore leads to a more linear load-extension behaviour. This explains the reason why there was no clear knee point in the Hoechst curve.

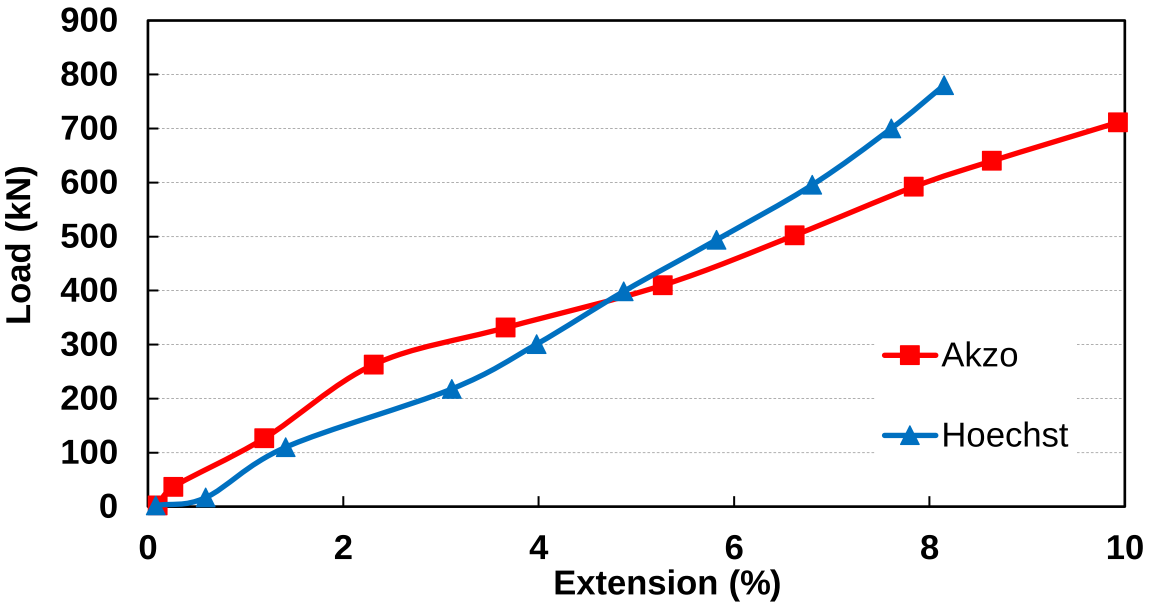

Fig. 10. Typical load-extension behaviour of 44mm Akzo and Hoechst rope tested with Stress Relief Socket.

The maximum extension at break for different constructions of Hoechst and Akzo materials including filament, yarn, strand, 18mm sub-rope and 44mm rope is shown graphically in Fig. 11. The results show that the maximum strain to failure is the same for all the small size filaments up to the strand construction. There is a sharp rise in the strand. This is due to the inherent increase in the twist in the construction. The reason for this phenomenon is that during the initial stages of loading, a significant proportion of the extension consists of untwisting before complete loading is taken up by the filaments.

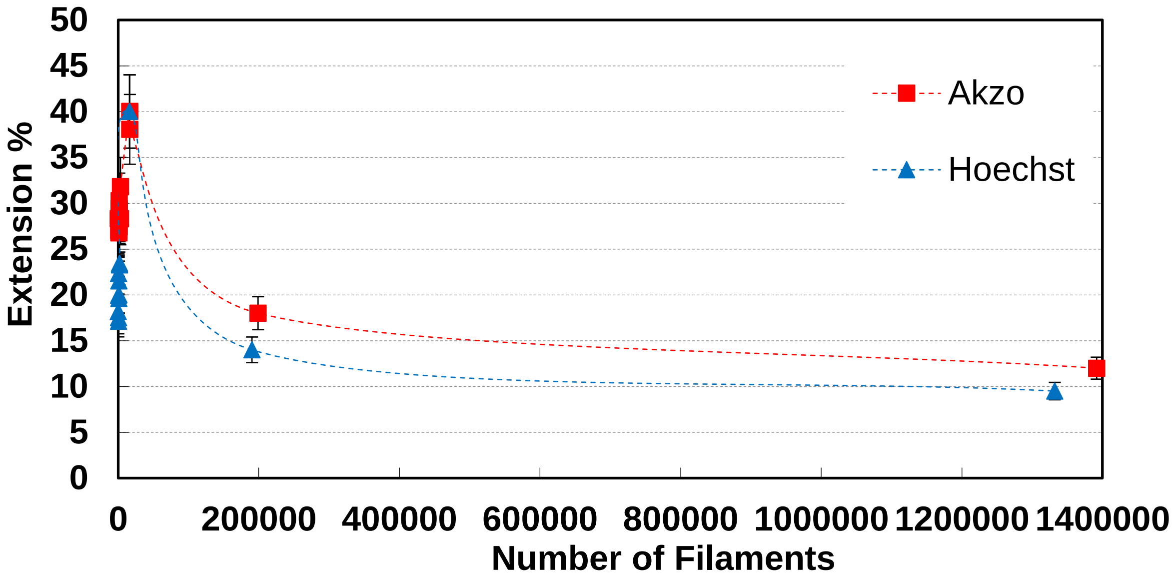

Fig. 11. Extension percentage at break for different number of filaments of Hoechst and Akzo materials.

3.4 Tensile strength of 120mm Rope

The main objective of all previous tests is to reach a resolution for terminating the 120mm rope, which is supposed to anchor oil platforms. Failures were observed to occur both near the sample ends and in the central section, no significant difference was noted for strengths corresponding to the two failure locations.

A breaking load of 4778 kN for 120mm Viking 7 rope was recorded. The results indicate that the breaking load for the 120mm rope is 5.8 times more than the 44mm rope while the difference in mass is 6.3 times. It is clear that when the rope size increases, the relative load bearing capability reduces. The relative efficiency for the different rope sizes is shown in Fig. 12. The 120mm rope achieved a breaking load efficiency of 78% compared with the filament-breaking load. It can be seen that efficiency is reduced at a faster rate up to 44mm rope size beyond which the efficiency levels off. Therefore, it is possible to achieve an approximate strength of the larger ropes from the smaller 44mm size. In order to develop a mathematical model to predict tensile performance of larger ropes consideration must be made to the following:

- Size and types of fibres,
- Construction of filaments, strands, and sub ropes
- Surface coating used on the fibres
- Types of termination used

The rope manufacturers usually consider at least a 50% reduction in the rope efficiency from filament to rope. Although 50% reduction might not be an acceptable figure for safe working condition, it is a proper method to show the capability of the rope and the advantage of termination over the other methods. The post-mortem examination of the rope indicated that 2 sub-ropes were still intact. Having some unbroken sub-rope indicates that a higher breaking load is expected if more care is taken in sample preparation and arrangement of the materials in the socket. Considering the first test on this rope with this termination and some unbroken sub-ropes, the results are promising and further work on this method is recommended.

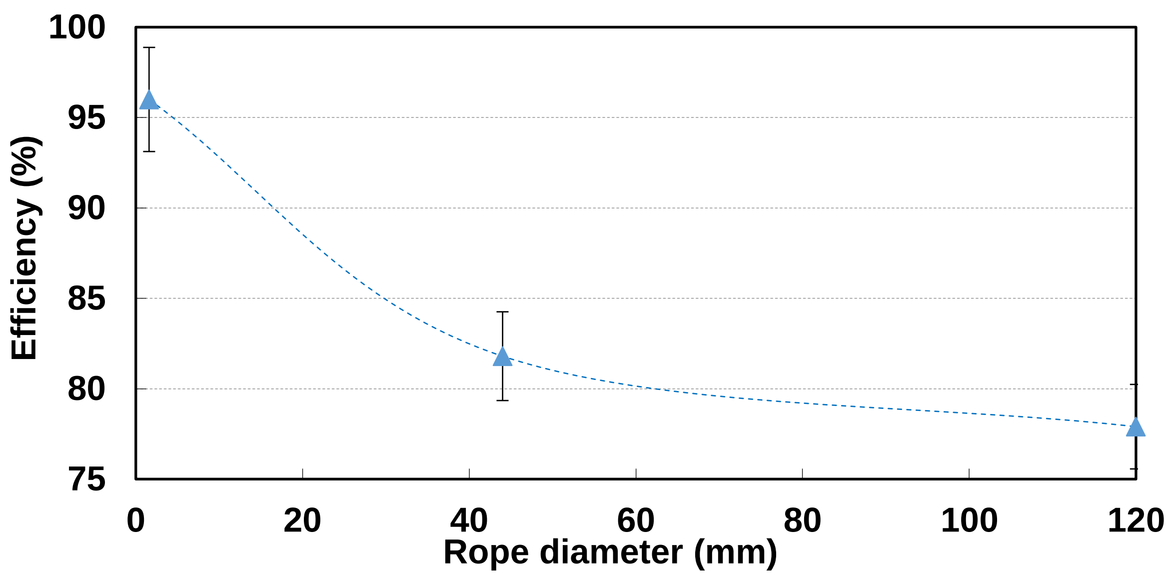

Fig. 12. Tensile efficiency drop by rope diameter using the Stress Relief Socket.

To measure the socket-draw and investigate the tenacity behaviour of the rope, three separate extension measurements were taken. These included machine displacement, i.e. face-to-face displacement of sockets as well as using two independent displacement sensors, namely nearside displacement (NSD) and offside displacement (OSD) transducers. Fig. 13 shows the load-extension curve for the 120mm rope sample with the transducers attached to the 2m gauge length of the rope.

The extension measurement was intentionally delayed by applying a preload of 500 kN to remove the effect of sub-ropes misalignment. Thus, when the pre-load is initially applied the alignment of sub ropes takes place and therefore no deformation of the rope material is expected during this period. This is indicated as a sharp rise in load with no change in displacement between 250-500 kN, the rope response is mostly structural in the initial stages of loading.

It can be seen that as the load increased, the machine displacement increased at a faster rate than the other two transducers. This is because the machine displacement is a combination of the machine stroke, socket draw, and rope extension while the transducers show rope extension only. The rope, as a textile structure, reacts to an applied stress with a combination of structural and material deformations. Its deformation, thus, depends on the structure of the fibre materials used. As a rigid structure, 120mm rope behaves like a metal bar when the load is fully transferred to the sub-ropes.

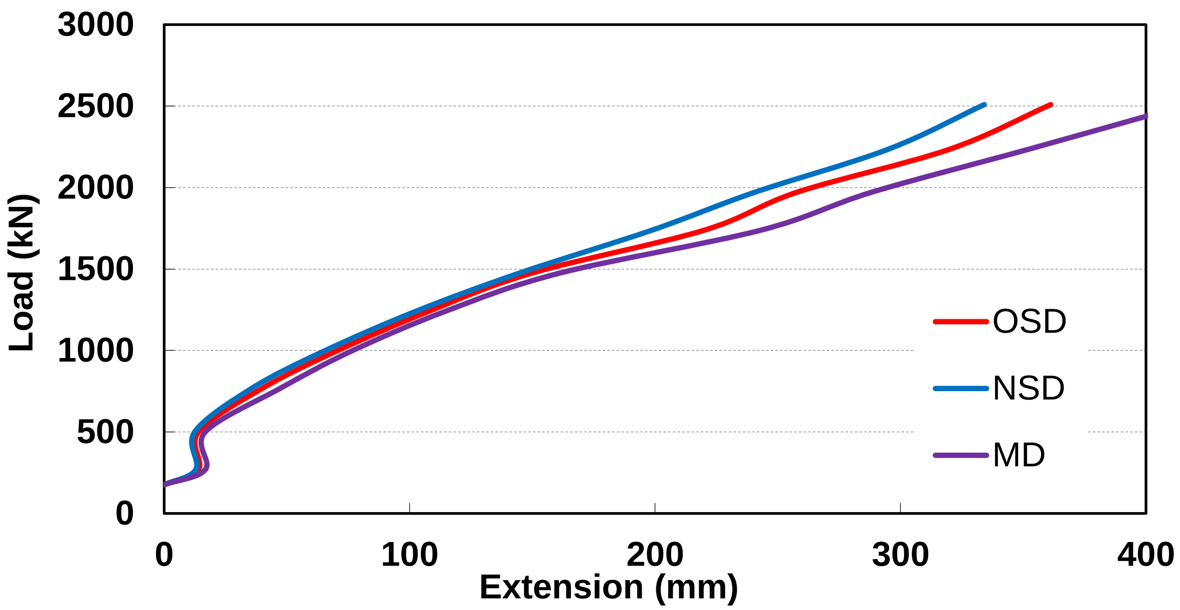

Fig 13. Typical load-extension profile for the 120mm rope samples. (OSD= Offside Displacement transducer; NSD= Nearside Displacement transducer; MD= Machine Displacement).

The mean extension values for the three rope sizes at the load of 2500kN are listed in Table 6. It can be observed that when the rope size increases, the extension drops dramatically, the extension decreases by 43% from 28mm rope to 44mm rope while in comparison with120mm rope the decrease in extension is about 72%.

Rope Type	**%Extension at 2500kN**
28mm rope (120mm sub-rope)	5.35
44mm rope	3.04
120mm rope	1.45

Table 6. Extension at constant load for different rope sizes.

The load-extension curve for 120mm rope until final break is presented in Fig. 14. The sample broke at 4778kN. Partial failure took place with two sub-ropes still intact. There is no clear knee point in the profile. Because most of the fibre realignment and socket-draw were removed in the previous cycling and tensioning processes. When the rope was made, it was expected that most of the fibres realignment is removed under the sub-ropes tension. Slight fluctuation in the graph around 3700kN is due to the progression of microdamage/ premature failure of subcomponents. The total extension in the rope was measured at 150.39mm. Socket face to face length after initial cycling was measured to be 334.22mm at 2500kN. A simple comparison between these two figures, indicate that most socket-draw and fibre realignments are removed during the loading regime before final break. Therefore the resultant extension is considered to be the actual extension of the rope excluding fibre realignments and socket-draw.

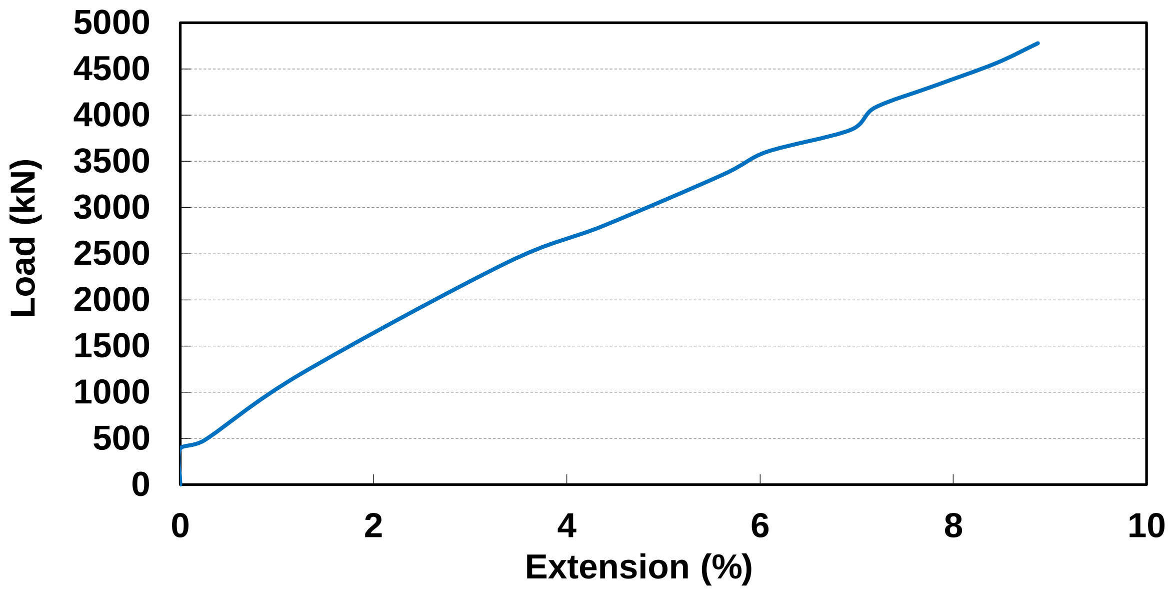

Fig. 14. Typical Load-Extension curve for 120mm rope.

It is desirable to develop a model to predict the strength of larger ropes from the smaller 44mm or 18mm sub ropes. Ali and Chouw (2013) have presented simple equations to predict tensile strength for different rope diameters, but their model is not comprehensive.

4. Conclusions

Traditional methods of rope termination for heavy-duty polyester ropes in MRE applications lead to premature failure due to high stress concentration areas around the termination. This always restricts the polyester ropes to reach their full potential and leads to early failure. However, further investigations are required for rope materials, size and termination configuration. This paper reports experimental results on the effects of two important parameters including materials and termination configuration on the detailed tensile performance of filaments, yarns, strands, sub-ropes, 44mm ropes and 120mm ropes. Several useful research outcomes have been obtained. These include:

- At higher applied load, the rate of tenacities in Akzo and Hoechst all decreased at similar extensions before they break, which takes place between 32% and 36% of strain. The main reason for decrease in the loading performance is filaments fusing together due to high temperature resulted from the high strain energy during the loading process.
- For the sub-rope, the rope tenacity for the Splice termination (566.7 mN/Tex for Akzo and 565.16 mN/Tex for Hoechst) is higher than that of Parafil (107.39 mN/Tex for Akzo and 113.43 mN/Tex for Hoechst) and the Stress Relief Socket (83.58 mN/Tex for Akzo and 81.57 mN/Tex for Hoechst) in both materials.
- The use of Stress Relief Socket leads to a reduction in high stress concentration areas inside the termination, which translates to tensile strength of the rope increases.
- The Stress Relief Socket was found to have improved Akzo rope performance 12.6% and Hoechst Rope by 5% compared to the splice methods.
- The advantage of Stress Relief Socket is more pronounced when it is used in 120 mm Akzo ropes
- For 120mm rope, the final break force and extension to failure values were measured to be 4778 kN and 150.39 mm respectively. It achieved a breaking load efficiency of 78% as compared with filament breaking load. Thus, the efficiency is reduced at a faster rate up to 44mm rope size beyond which the efficiency levels off.

Acknowledgements

The authors would like to acknowledge the support of the lead author through Industrial Research Programme, which was fully funded by Bridon Marine.

References:

Ali, M and Chouw, N 2013 Experimental investigations on coconut-fibre rope tensile strength and pullout from coconut fibre reinforced concrete, Construction and Building Materials 41, 681–690

Alwis, K.G.N.C., Burgoyne, C.J., 2008. Accelerated creep testing for aramid fibres using the stepped isothermal method. J. Mater. Sci. https://doi.org/10.1007/s10853-008-2676-0

Bashir, I., Walsh, J., Thies, P.R., Weller, S.D., Blondel, P., Johanning, L., 2017. Underwater acoustic emission monitoring – Experimental investigations and acoustic signature recognition of synthetic mooring ropes. Appl. Acoust. https://doi.org/10.1016/j.apacoust.2017.01.033

Beltrán, J.F., De Vico, E., 2015. Assessment of static rope behavior with asymmetric damage distribution. Eng. Struct. https://doi.org/10.1016/j.engstruct.2014.12.026

Bunsell, A. R, 2018 Handbook of Properties of Textile and Technical Fibres, Elsevier Science, ISBN:0081012721, 9780081012727

Chaplin, C.R., 1999. Torsional failure of a wire rope mooring line during installation in deep water. Eng. Fail. Anal. https://doi.org/10.1016/S1350-6307(98)00043-0

Chiao, C.C., Moore, R.L., Chiao, T.T., 1977. Measurement of shear properties of fibre composites. Part 2. Shear properties of an aramid fibre in several epoxy resins. Composites. https://doi.org/10.1016/0010-4361(77)90012-X

Davies, P., Reaud, Y., Dussud, L., Woerther, P., 2011. Mechanical behaviour of HMPE and aramid fibre ropes for deep sea handling operations. Ocean Eng. 38 (17), 2208–2214. https://doi.org/10.1016/j.oceaneng.2011.10.010

Davies, P., François, M., Lacotte, N., Vu, T.D., Durville, D., 2015. An empirical model to predict the lifetime of braided HMPE handling ropes under cyclic bend over sheave (CBOS) loading. Ocean Eng. https://doi.org/10.1016/j.oceaneng.2015.01.003

Drummond, G., Watson, J.F., Acarnley, P.P., 2007. Acoustic emission from wire ropes during proof load and fatigue testing. NDT E Int. https://doi.org/10.1016/j.ndteint.2006.07.005

Glaser, R., Moore R., Chiao T., 1984. Life Estimation of Aramid/Epoxy Composites Under Sustained Tension, Journal of Composites, Technology and Research. https://doi.org/10.1520/CTR10881J

Health and Safety Executive Research report 444. Floating production system, JIP FPS mooring integrity. Prepared by Noble Denton Europe Limited; 2006.

Heirigs, L.T., Schwartz, P., 1992. Properties of Small Diameter Aramid Double Braids: Fatigue Lifetime, Strength Retention after Abrasion, and Strength Modeling. Text. Res. J. https://doi.org/10.1177/004051759206200706

Huang, W., Liu, H., Lian, Y., Li, L., 2013. Modeling nonlinear creep and recovery behaviors of synthetic fiber ropes for deepwater moorings. Appl. Ocean Res. https://doi.org/10.1016/j.apor.2012.10.004

Gordelier, T., Parish, D., Thies, P.R., Weller, S., Davies, P., Le Gac, P.Y., Johanning, L., 2018. Assessing the performance durability of elastomeric moorings: Assembly investigations enhanced by sub-component tests. Ocean Eng. https://doi.org/10.1016/j.oceaneng.2018.02.014

Lafitte, M.H., Bunsell, A.R., 1982. The fatigue behaviour of Kevlar-29 fibres. J. Mater. Sci. https://doi.org/10.1007/BF00543749

Leal, A.A., Stämpfli, R., Hufenus, R., 2017. On the analysis of cut resistance in polymer-based climbing ropes: New testing methodology and resulting modes of failure. Polym. Test. https://doi.org/10.1016/j.polymertesting.2017.07.004

Lee, K.H., Han, H.S., Park, S., 2015. Failure analysis of naval vessel's mooring system and suggestion of reducing mooring line tension under ocean wave excitation. Eng. Fail. Anal. https://doi.org/10.1016/j.engfailanal.2015.08.005

Lian, Y., Liu, H., Huang, W., Li, L., 2015. A creep-rupture model of synthetic fiber ropes for deepwater moorings based on thermodynamics. Appl. Ocean Res. https://doi.org/10.1016/j.apor.2015.06.009

Lian, Y., Liu, H., Zhang, Y., Li, L., 2017. An experimental investigation on fatigue behaviors of HMPE ropes. Ocean Eng. https://doi.org/10.1016/j.oceaneng.2017.05.007

Lian, Y., Liu, H., Li, L., Zhang, Y., 2018. An experimental investigation on the bedding-in behavior of synthetic fiber ropes. Ocean Eng. https://doi.org/10.1016/j.oceaneng.2018.04.071

Liu, H., Huang, W., Lian, Y., Li, L., 2014. An experimental investigation on nonlinear behaviors of synthetic fiber ropes for deepwater moorings under cyclic loading. Appl. Ocean Res. https://doi.org/10.1016/j.apor.2013.12.003

Mousavi, M.E., Gardoni, P., Maadooliat, M., 2013. Progressive reliability method and its application to offshore mooring systems. Eng. Struct. https://doi.org/10.1016/j.engstruct.2013.08.016

Natural Disaster Organization, 1996. Disaster Rescue-Australian Emergency Manual, ISBN 0 642 25611 X

Paton, A.G., Casey, N.F., Fairbairn, J., Banks, W.M., 2001. Advances in the fatigue assessment of wire ropes. Ocean Eng. https://doi.org/10.1016/S0029-8018(00)00014-7

Peterka, P., Krešák, J., Kropuch, S., Fedorko, G., Molnar, V., Vojtko, M., 2014. Failure analysis of hoisting steel wire rope. Eng. Fail. Anal. https://doi.org/10.1016/j.engfailanal.2014.06.005

Rivera, F.G., Edwards, G., Eren, E., Soua, S., 2018. Acoustic emission technique to monitor crack growth in a mooring chain. Appl. Acoust. https://doi.org/10.1016/j.apacoust.2018.04.034

Singh, R.P., Mallick, M., Verma, M.K., 2016. Studies on failure behaviour of wire rope used in underground coal mines. Eng. Fail. Anal. https://doi.org/10.1016/j.engfailanal.2016.09.002

Suh, J.I., Chang, S.P., 2000. Experimental study on fatigue behaviour of wire ropes. Int. J. Fatigue. https://doi.org/10.1016/S0142-1123(00)00003-7

Weller, S.D., Johanning, L., Davies, P., Banfield, S.J., 2015. Synthetic mooring ropes for marine renewable energy applications. Renew. Energy. https://doi.org/10.1016/j.renene.2015.03.058

Weller, S.D., Davies, P., Vickers, A.W., Johanning, L., 2015. Synthetic rope responses in the context of load history: The influence of aging. Ocean Eng. https://doi.org/10.1016/j.oceaneng.2014.12.013

Wu, H.C., Seo, M.H., Backer, S., Mandell, J.F., 1995. Structural Modeling of Double-Braided Synthetic Fiber Ropes. Text. Res. J. https://doi.org/10.1177/004051759506501101

Xu, T.J., Zhao, Y.P., Dong, G.H., Bi, C.W., 2014. Fatigue analysis of mooring system for net cage under random loads. Aquac. Eng. https://doi.org/10.1016/j.aquaeng.2013.10.004

Zhang, X., Sun, L., Ma, C., Fassezke, E., Sun, H., 2016. A reliability evaluation method based on the weakest failure modes for side-by-side offloading mooring system of FPSO. J. Loss Prev. Process Ind. https://doi.org/10.1016/j.jlp.2016.03.011